PHYSICAL REVIEW A **92**, 051403(R) (2015)

Creation and survival of autoionizing states in strong laser fields

Lutz Fechner,[1,*] Nicolas Camus,[1] Andreas Krupp,[1] Joachim Ullrich,[1,2] Thomas Pfeifer,[1] and Robert Moshammer[1,†]
[1]*Max-Planck-Institut für Kernphysik, Saupfercheckweg 1, 69117 Heidelberg, Germany*
[2]*Physikalisch-Technische Bundesanstalt, Bundesallee 100, 38116 Braunschweig, Germany*
(Received 3 June 2015; published 30 November 2015)

Very sharp, low-energy structures observed in photoelectron spectra reveal the population of autoionizing states in krypton and argon in strong laser fields over a large range of different wavelengths. The energies of the electrons, emitted by autoionization in a field-free environment, provide direct information about the spectrum of states involved. Despite their ability to resist ionization by the populating laser pulse, we demonstrate the possibility to promote the excited electrons into the continuum by subsequent absorption of a single photon. Thus, applying a classical pump-probe scheme, we are able to manipulate the autoionization contribution on a picosecond time scale. Different scenarios for the creation of autoionizing states in strong laser fields are discussed.

DOI: 10.1103/PhysRevA.92.051403 PACS number(s): 32.80.Fb, 32.80.Rm, 32.80.Zb

Within the framework of single-electron theory for strong-field ionization [1–4] a wealth of experimental observations, as e.g., the rates for single ionization [5] or photoelectron energy spectra [6] and angular distributions [7], are predicted reasonably well. However, many phenomena, such as the enhancement of double ionization at low intensities [8,9], require extensions to and refinements of these models. In particular, the electronic structure of the parent ion [10,11] and the electron dynamics in the combined laser electric and atomic Coulomb field [12,13] turned out to play a crucial role. Both aspects were needed to explain the recently discovered neutral exit channel [14,15], dubbed frustrated tunneling ionization (FTI). There, involving the famous three-step model [16], a highly excited neutral atom is formed by the recapture of a low-energy electron recolliding with the parent ion. Although the neutral atom is directly detectable in specifically designed experiments [14], the proof of this process often requires additional experimental effort, e.g., subsequent field ionization of the excited atoms [14,17].

In this Rapid Communication we report on the observation of very sharp, low-energy structures in the photoelectron spectra observed for strong-field ionization of krypton and argon at different wavelengths. The energetic widths of the peaks are in the meV range and thus smaller than the spectral width of the laser ($\gtrsim$45 meV) and far smaller than the ponderomotive potential ($>$17 eV at 790 nm and 3×10^{14} W/cm^2). We prove the appearance of the low-energy electrons over a large range of wavelengths and show that they originate from autoionization of the neutral species, long after the laser pulse. From this we infer the existence of a mechanism which efficiently populates autoionizing states in krypton and argon in strong laser fields. Moreover, our measurements reveal the spectrum of the strong-field excited states. Different population scenarios and a possible connection to the well-known dielectronic recombination processes (see, e.g., [18–20], and references therein) are discussed. Finally, we unambiguously demonstrate that—although the highly excited autoionizing states may resist ionization by the laser pulse—it is possible to manipulate the population with a second, much weaker probe pulse.

*lutz.fechner@mpi-hd.mpg.de
†robert.moshammer@mpi-hd.mpg.de

The experimental setup consists of a laser system delivering strong femtosecond pulses with a duration of $\lesssim$30 fs at a central wavelength of about 790 nm. A commercial optical parametric amplifier is used for shifting the central wavelength in the range from 470 to 1600 nm. The intensity used in the experiments is estimated to be on the order of 3×10^{14} W/cm^2; the pulse durations are typically 20 fs or longer. For the pump-probe measurements at 790 nm, a beam splitter and a piezodriven Mach-Zehnder interferometer are used. We apply an asymmetric intensity splitting, namely, 90% as pump and 10% as probe pulse. The laser pulses are focused into a reaction microscope (REMI) with a background pressure in the low 10^{-11} mbar regime. Atoms from a very dilute supersonic gas jet are ionized and the created ions and electrons are accelerated in combined electric and magnetic fields. From their flight times and the impact positions on the respective detectors, the trajectories of the particles and thus their initial momentum vectors are reconstructed with very high precision (see, e.g., [21] for details).

The upper part of Fig. 1 displays two high-resolution photoelectron momentum distributions (PMD) from a series of measurements performed with krypton and argon at different wavelengths. $p_\parallel$ denotes the momentum component along the laser polarization and $p_{\mathrm{tr}} = (p_x^2 + p_y^2)^{1/2}$ the transverse one. Exploiting the coincidence capability of the REMI, all features discussed are proven to stem from single ionization of the respective target. In regions of larger momenta, typical features arising from inter- and intracycle interference of electron trajectories [22] are visible, including the characteristic and broad equienergetic rings representing above-threshold ionization (see, e.g., [11], and references therein). While these patterns are very pronounced in the PMD recorded for short wavelengths they wash out as the ponderomotive potential increases towards long wavelengths. However, also for the longest wavelength used, 1600 nm, faint residuals of the features are visible. In addition, we observe sharp Freeman resonances [10,11], indicating ionization via singly excited states.

In the following we focus on the regions of very low electron momenta in the PMD, magnified in the lower part of Fig. 1. For both targets, krypton and argon, a series of sharp rings can be observed, indicating the emission of electrons with very low, but well-defined kinetic energies. For krypton, up to four or even five rings are visible with decreasing distance between

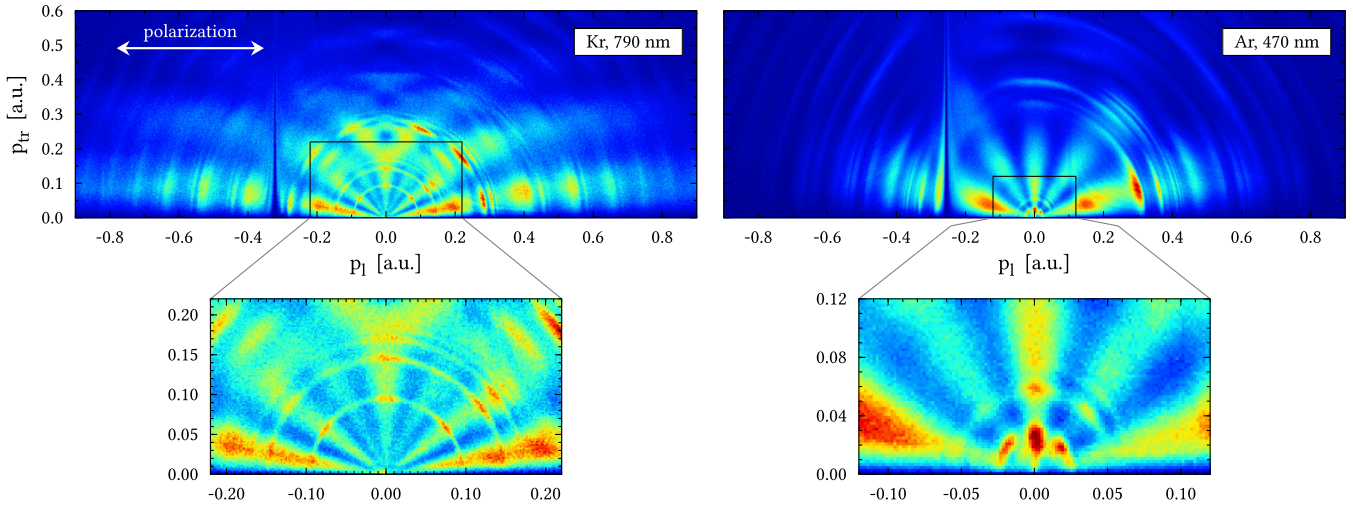

FIG. 1. (Color online) Typical PMD obtained for the ionization of krypton (left) and argon (right). The laser polarization is aligned along the horizontal axes; linear color scales are used. In each of the magnified regions, a series of sharp rings is visible, most clearly for krypton. The total momentum of these electrons—and likewise their kinetic energy—is observed to be independent of the wavelength used for ionization (see text).

them for increasing radii. In the case of argon, the observed rings are less pronounced and even lower in energy.

For closer inspection of the rings we plot the photoelectron energy spectra (PES) (see Fig. 2), where each ring forms a sharp peak. The experimental data is represented by colored bars; solid lines are fits to the data, consisting of a broad Gaussian distribution to account for the background and several sharp pseudo-Voigt peaks [23]. The observed peak positions in the 470 nm data recorded with krypton were utilized for a linear calibration of the experimental momenta, applied to all data sets displayed. This calibration has been considered already for Fig. 1. In striking contrast to the Freeman resonances, the positions of the observed low-energy peaks in Fig. 2 are independent of the wavelength. This is only reasonable, if the electrons are emitted at an instant when no laser field is present, that is, at a time when the laser pulse is already over. However, it requires the preparation of a state in which the total energy exceeds the ionization potential of the system but—at first instance—the electrons are still bound. In the states relevant for our experiment, one electron is found in a high-lying Rydberg state orbiting the residual, singly charged ion. The latter may be found either in its $^2P_{3/2}$ ground state (I^+) or in the spin-orbit excited $^2P_{1/2}$ state (I^{+*}), which results in a situation as outlined above: The spin-orbit splitting ΔE between these states is about 666 and 177 meV in Kr^+ and Ar^+, respectively [24]. This amount of energy—stored in the inner ionic core of the system and released upon its relaxation—is enough to overcome many of the Rydberg binding energies and thus will lead to the emission of the outer electron via autoionization [25]. Due to the simultaneous presence of two excitations in the atom, namely, the electronic Rydberg excitation and the spin-orbit excitation of the ionic core, we refer to these states as doubly excited states (DES) in the following. They have been extensively studied in recent years (see [26], and references therein).

The energy of the Rydberg electron in a state characterized by the principal quantum number n and the angular momentum quantum number l can be described in terms of the general Rydberg series [25]

$$E_{n,l}^{(*)} = E_i^{(*)} - \mathcal{R}_\infty/(n+\delta_l)^2, \tag{1}$$

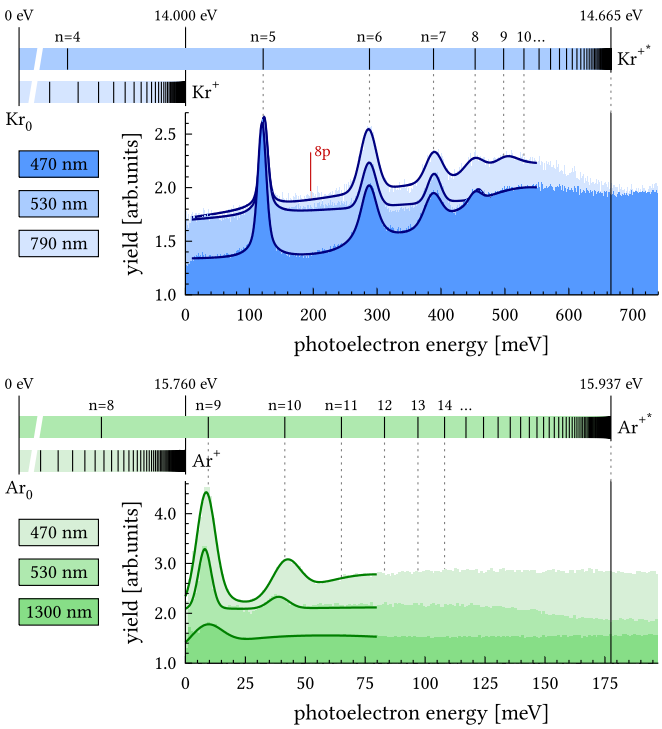

FIG. 2. (Color online) Energy spectra of low-energy photoelectrons for ionization of krypton (top) and argon (bottom) at different wavelengths. The solid lines represent simple fits to the data; theoretical energy levels are calculated with Eq. (1) and $\delta_l \equiv 0$ (see text). Additionally, the reference position of the $8p$ DES in krypton is displayed, taken from [24]. The peak positions in the 470 nm data recorded with krypton were utilized for calibration of all spectra shown (see text).

where $E_i^{(*)}$ is the respective ionization potential for ionization to a bare I^+ or I^{+*} ion and $\mathcal{R}_\infty$ denotes the Rydberg constant. δ_l is the quantum defect, considering the partial screening of the nuclear charge due to the finite probability density close to the nucleus. It is significant only for states with small l and quickly approaches zero for larger values. Thus, Eq. (1) with $\delta_l \equiv 0$ yields a simplified level diagram for the Rydberg series, which is a very good approximation for all states with large angular momentum. In Fig. 2, these diagrams are displayed for krypton as well as for argon. For $n \geqslant 5$ (krypton) and $n \geqslant 9$ (argon), the total energy of the Rydberg states in the presence of the excited ionic core exceeds the ionization potential into the ground-state ion. These DES decay via autoionization and produce electrons with well-defined energies, smaller than the spin-orbit splitting of the system [25]. The energies E_n^* calculated with Eq. (1) and $\delta_l \equiv 0$ significantly differ from the available spectroscopic data [24] for $l < 3$ and $l < 2$ for the case of krypton and argon, respectively. For larger l, the deviations are on the order of a few meV and below.

Very good agreement between the full series of peaks with the predicted energies can be observed for all spectra shown in Fig. 2. Besides providing a direct proof of the population of DES in strong laser fields over a large range of wavelengths, our results additionally yield state-selective information. In this regard, the absence of any peak not covered by the simplified level diagram is noteworthy. It allows the conclusion, that the emission of electrons with sharp, well-defined energies is limited to states with $l \geqslant 3$ and $l \geqslant 2$ in krypton and argon, respectively. All other states, e.g., the $8p$ DES of krypton additionally displayed in Fig. 2, are not significantly active in this respect. Before possible reasons are discussed, we note the additional presence of a "plateau" region in the PES for krypton, falling off towards the ionization potential of Kr^{+*}. In this region, for $n \geqslant 9$, the energy difference between adjacent states becomes comparable with the typical width of the peaks such that they cannot be resolved anymore. The same behavior may—less pronounced—also be visible for argon at 530 nm. The peak widths observed we attribute to the experimental resolution rather than being related to the lifetime of the states.

The fact that only a subset of states contributes to the series of peaks in the PES may be understood either as a consequence of the population process or the autoionization dynamics. The experimental finding calls for a favored population of states with $l \geqslant 3$ and $l \geqslant 2$ in krypton and argon, respectively. However, assuming equal population of all states, peaks covered by the simplified level diagram are expected to be enhanced by the contribution of several, essentially degenerated l states. With regard to the autoionization process, the absence of signal from low-l states may also be caused by short autoionization lifetimes. If the electrons are emitted at a time when the laser field is still present, the respective peaks are expected to be broadened on an energy scale of the ponderomotive potential, which is much larger than their initial width or their separation. Thus, these states would contribute to the broad background instead of leaving sharp peaks in the PES as a footprint.

In the tunneling regime, the mechanism of FTI has recently been discussed as a possible population scenario for (singly excited) Rydberg states [14,15]. In this process, a low-energy recollision of a tunnel-ionized electron with its parent ion forms a neutral Rydberg atom. Within this picture, two different sequences are possible which may lead to the population of DES. First, the electron may tunnel out, directly leaving the ionic core in the excited $^2P_{1/2}$ state. Such an excitation of the residual core by tunnel ionization is indeed possible and can even be utilized, e.g., in order to create a coherent superposition of the ionic ground and the excited state [27–32]. Later, the freed electron may recollide with the excited ion and be recaptured. Alternatively, the electron may first tunnel, leaving the residual ion in its ground state. Later, after being driven in the laser field, the electron can be resonantly recaptured into a Rydberg state, simultaneously using its excess energy to resonantly excite the ionic core. Such processes are well known from dielectronic recombination experiments (see, e.g., [18–20], and references therein) and have been largely investigated, e.g., in ion storage-ring experiments for higher charged or lighter ions [18]. To the best of our knowledge, such experiments have never been performed for singly charged argon or krypton.

The ability of the DES to resist ionization by the laser field until the pulse is over and autoionization takes place raises the question: If and to what extent is their population accessible in a classical pump-probe experiment, using a second laser pulse for inspection? With krypton as a target, we use 90% of the pulse intensity to populate the DES and only 10% for probing the system. Thus, the probe pulse alone is not intense enough to cause significant ground-state ionization. In order to achieve better statistical significance, the time delay between the pulses has been changed in discrete steps rather than scanning it continuously. A reference spectrum has been recorded at a negative time delay of about −80 fs, where the weak probe pulse precedes the strong pump pulse. We assume that this

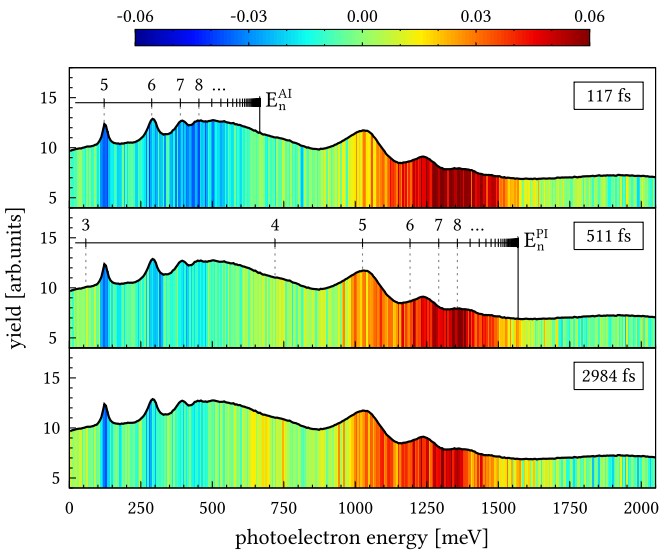

FIG. 3. (Color online) Results of the pump-probe measurements with krypton. The solid black line (identical in all plots) represents the delay-averaged PES. Positions of the autoionization peaks are denoted by E_n^{AI}; expected electron energies E_n^{PI} for the photoionization channel are additionally displayed (see text). The relative differences between PES obtained at different time delays and the reference PES are encoded in the colored filling below the curves (see text).

configuration leaves the target in its ground state before the pump pulse arrives: The reference spectrum thus is effectively created by the pump pulse alone.

The black solid line shown in all three panels of Fig. 3 represents the delay-averaged PES. Again, the peaks created by autoionization are found in the energy range below ≈ 666 meV and are used for absolute calibration as before. The relative difference between the PES obtained at a certain time delay and the reference PES, i.e., the difference between the normalized PES and the normalized reference PES divided by the latter, is encoded in the colors of the filling below the curves: Blue colors indicate regions where the signal is suppressed by the probe pulse, and red colors those where it is enhanced. Figure 3 shows the results for three selected time delays, up to about 3 ps. In all cases, a suppression of the autoionization peaks can be observed. Rather than being emitted by autoionization, the Rydberg electrons are freed from the Kr^{+*} core by absorption of a photon in the probe pulse. The expected photoelectron energies $E_n^{\mathrm{PI}} = \hbar\omega - \mathcal{R}_\infty/n^2$ are shown together with the data in the second panel of Fig. 3 and fall in the region filled with red colors, indicating probe-pulse-induced enhancement of signal. In contrast to the sharp peaks originating from autoionization in a field-free environment, the structures created in the presence of the probe pulse and its ponderomotive potential show the characteristic broadening.

The overall effect measured is small with relative differences in the order of only a few percent. Nevertheless, with increasing time delay along the three panels of Fig. 3, the influence of the probe pulse on the PES can be observed to decrease. At large delays, a significant part of the DES populated in the pump pulse has already undergone autoionization before the probe pulse arrives. While the contrast obtained and, in particular, the changes with the time delay are too small for a quantitative determination of the lifetimes, the result is consistent with the observed width of the autoionization peaks, requiring lifetimes longer than the laser pulse duration.

In conclusion, our results prove the population of DES in neutral krypton and argon atoms by strong laser fields over a large range of wavelengths. Since the doubly excited atoms autoionize in a field-free environment, long after the laser pulse is over, sharp, low-energy peaks are formed in the respective PES, revealing state-selective information about the states involved: We find $l \geqslant 3$ and $l \geqslant 2$ for krypton and argon, respectively, while all other states are absent in the PES. Moreover, we demonstrate the general accessibility of the states in a classical pump-probe scheme on a picosecond time scale. With regard to the recently discovered population of singly excited states by FTI, future work may focus on the observed additional excitation of the ionic core and elucidate the individual contribution of the two population scenarios discussed.

[1] L. V. Keldysh, Zh. Eksp. Teor. Fiz. **47**, 1945 (1965) [Sov. Phys. JETP **20**, 1307 (1965)].
[2] A. M. Perelomov, V. S. Popov, and M. V. Terent'ev, Zh. Eksp. Teor. Fiz. **50**, 1393 (1966) [Sov. Phys. JETP **23**, 924 (1966)].
[3] M. V. Ammosov, N. B. Delone, and V. P. Krainov, Zh. Eksp. Teor. Fiz. **91**, 2008 (1986) [Sov. Phys. JETP **64**, 1191 (1986)].
[4] K. C. Kulander, K. J. Schafer, and J. L. Krause, Int. J. Quantum Chem. **40**, 415 (1991).
[5] S. Augst, D. D. Meyerhofer, D. Strickland, and S. L. Chin, J. Opt. Soc. Am. B **8**, 858 (1991).
[6] K. J. Schafer, B. Yang, L. F. DiMauro, and K. C. Kulander, Phys. Rev. Lett. **70**, 1599 (1993).
[7] B. Yang, K. J. Schafer, B. Walker, K. C. Kulander, P. Agostini, and L. F. DiMauro, Phys. Rev. Lett. **71**, 3770 (1993).
[8] A. L'Huillier, L. A. Lompre, G. Mainfray, and C. Manus, Phys. Rev. Lett. **48**, 1814 (1982).
[9] B. Walker, B. Sheehy, L. F. DiMauro, P. Agostini, K. J. Schafer, and K. C. Kulander, Phys. Rev. Lett. **73**, 1227 (1994).
[10] R. R. Freeman, P. H. Bucksbaum, H. Milchberg, S. Darack, D. Schumacher, and M. E. Geusic, Phys. Rev. Lett. **59**, 1092 (1987).
[11] R. R. Freeman and P. H. Bucksbaum, J. Phys. B **24**, 325 (1991).
[12] S. Basile, F. Trombetta, and G. Ferrante, Phys. Rev. Lett. **61**, 2435 (1988).
[13] T. Brabec, M. Y. Ivanov, and P. B. Corkum, Phys. Rev. A **54**, R2551(R) (1996).
[14] T. Nubbemeyer, K. Gorling, A. Saenz, U. Eichmann, and W. Sandner, Phys. Rev. Lett. **101**, 233001 (2008).
[15] A. S. Landsman, A. N. Pfeiffer, C. Hofmann, M. Smolarski, C. Cirelli, and U. Keller, New J. Phys. **15**, 013001 (2013).
[16] P. B. Corkum, Phys. Rev. Lett. **71**, 1994 (1993).
[17] R. R. Jones, D. W. Schumacher, and P. H. Bucksbaum, Phys. Rev. A **47**, R49(R) (1993).
[18] S. Schippers, J. Phys.: Conf. Ser. **163**, 012001 (2009).
[19] C. Beilmann, P. H. Mokler, S. Bernitt, C. H. Keitel, J. Ullrich, J. R. Crespo Lopez-Urrutia, and Z. Harman, Phys. Rev. Lett. **107**, 143201 (2011).
[20] Y. Hahn and K. J. LaGattuta, Phys. Rep. **166**, 195 (1988).
[21] J. Ullrich, R. Moshammer, A. Dorn, R. Dörner, L. P. H. Schmidt, and H. Schmidt-Böcking, Rep. Prog. Phys. **66**, 1463 (2003).
[22] D. G. Arbó, K. L. Ishikawa, E. Persson, and J. Burgdörfer, Nucl. Instrum. Methods Phys. Res., Sect. B **279**, 24 (2012).
[23] G. K. Wertheim, M. A. Butler, K. W. West, and D. N. E. Buchanan, Rev. Sci. Instrum. **45**, 1369 (1974).
[24] A. Kramida, Y. Ralchenko, and J. Reader, and NIST ASD Team (2014), NIST Atomic Spectra Database (ver. 5.2), National Institute of Standards and Technology, Gaithersburg, MD, http://physics.nist.gov/asd.
[25] A. Muhlpfordt and U. Even, J. Chem. Phys. **103**, 4427 (1995).
[26] V. L. Sukhorukov, I. D. Petrov, M. Schäfer, F. Merkt, M.-W. Ruf, and H. Hotop, J. Phys. B **45**, 092001 (2012).
[27] N. Rohringer and R. Santra, Phys. Rev. A **79**, 053402 (2009).
[28] E. Goulielmakis, Z.-H. Loh, A. Wirth, R. Santra, N. Rohringer, V. S. Yakovlev, S. Zherebtsov, T. Pfeifer, A. M. Azzeer, M. F. Kling, S. R. Leone, and F. Krausz, Nature (London) **466**, 739 (2010).
[29] H. J. Wörner and P. B. Corkum, J. Phys. B **44**, 041001 (2011).
[30] A. Fleischer, H. J. Wörner, L. Arissian, L. R. Liu, M. Meckel, A. Rippert, R. Dörner, D. M. Villeneuve, P. B. Corkum, and A. Staudte, Phys. Rev. Lett. **107**, 113003 (2011).
[31] A. Wirth, M. T. Hassan, I. Grguraš, J. Gagnon, A. Moulet, T. T. Luu, S. Pabst, R. Santra, Z. A. Alahmed, A. M. Azzeer, V. S. Yakovlev, V. Pervak, F. Krausz, and E. Goulielmakis, Science **334**, 195 (2011).
[32] L. Fechner, N. Camus, J. Ullrich, T. Pfeifer, and R. Moshammer, Phys. Rev. Lett. **112**, 213001 (2014).